Nanostructure in block copolymer solutions: Rheology and small-angle neutron scattering

Jean-Pierre Habas, Emmanuel Pavie, and Christelle Perreur
Laboratoire de Physico-Chimie des Polymères UMR 5067, Université de Pau et des Pays de l'Adour, Avenue de l'Université, 64000 Pau, France

Alain Lapp
Laboratoire Léon Brillouin CEA Saclay, 91191 Gif-sur-Yvette Cedex, France

Jean Peyrelasse*
Laboratoire de Physico-Chimie des Polymères UMR 5067, Université de Pau et des Pays de l'Adour, Avenue de l'Université, 64000 Pau, France

(Received 9 February 2004; revised manuscript received 6 July 2004; published 20 December 2004)

Triblock copolymers composed of poly(ethylene oxide) (PEO) and poly(propylene oxide) (PPO) present an amphiphilic character in aqueous solutions. Since PPO is less hydrophilic than PEO and since their solubilities decrease when the temperature increases, the copolymers self-assemble spontaneously, forming micelles at moderate temperatures. For higher temperatures or concentrations, the copolymers or the micelles are ordered because of repulsive interactions and form lyotropic liquid crystalline phases. These are phases of very great viscosity with the aspect of gels, and transitions between different crystalline phases can occur at fixed concentration during an increase of temperature. We studied solutions of three different copolymers. The first two have a star structure. They are both composed of four branches $(EO)_x(PO)_y$ fixed on an ethylene diamine, but differ by the values of x and y. Their commercial name is Tetronic 908 ($x=114$, $y=21$) and Tetronic 704 ($x=16$, $y=18$). The third copolymer $(EO)_{37}(PO)_{56}(EO)_{37}$ is linear and is known under the name of Pluronic P105. The measurements of the shear complex elastic modulus according to the temperature is used to determine the temperatures of the different transitions. Then, small-angle neutron scattering on samples under flow and true crystallographic arguments make it possible to identify the nature of the crystalline phases. For the systems studied, we show that the branched copolymers form only one type of liquid crystalline phase, which is bcc for the T908 and lamellar for the T704. For the linear copolymer, it is possible to identify three transitions: micellar solution to hexagonal phase, hexagonal phase to body-centered cubic phase, and finally body-centered cubic phase to lamellar phase.

DOI: 10.1103/PhysRevE.70.061802 PACS number(s): 61.25.Hq, 61.12.Ld, 61.12.Ex

I. INTRODUCTION

Over the last few years, many studies have been performed on solutions of hydrosoluble associative copolymers. There are various kinds of associative copolymers, but all consist of at least two sequences whose solubilities in water become gradually very different—for example, during an increase in temperature. Because of their amphiphilic character, these polymers in solution form micelles. The most studied systems are probably triblock poly(ethylene oxide)-poly(propylene oxide)-poly(ethylene oxide) (PEO-PPO-PEO) in water [1–13], but also in organic solvents [14–16] or water/organic solvents mixtures [17–20]. Many studies have also been carried out on the influence of various additives [21–24]. Some researches report the physicochemical behavior of PPO-PEO-PPO copolymers [25–27] in aqueous solutions. Other studies are devoted to solutions of branched copolymers of PEO-PPO-PEO [28,29] or hydrophobically modified poly(oxyethylene) [30]. Various diblock copolymers [31,32] have also been widely studied, such as poly(oxyethylene)-poly(oxybutylene). For solutions in water or in polar solvents, in the liquid zone of the phase diagram, the micelles consist of a hydrophobic core surrounded by a layer containing more or less solvent. From small-angle neutron scattering (SANS) measurements, various models [1–5,14,18,21,24–26,28,29], assuming spherical micelles with two or three layers, can provide precise information about their structure: radius, volume fraction, aggregation number, etc. With many compounds, zones of very high viscosity, where the sample looks like a gel, can be found in the temperature-concentration diagram. In that case, the copolymers or the micelles are ordered because of repulsive interactions and form lyotropic liquid crystalline phases. Depending on the polymers studied or experimental conditions (temperature, concentration), very diverse structures are described. In many cases, the micelles condense according to a cubic lattice [17,26,29], but the polymer can also form wormlike micelles [21], hexagonally packed cylindrical micelles [13,20,22], lamellar structures [22], or gyroid phases [33,34]. The possibility of transitions between some of these structures often induces a great deal of confusion in the literature. The case of Pluronic F127 ($EO_{100}PO_{70}EO_{100}$ where EO is ethylene oxide and PO propylene oxide) is exemplary. Prud'homme *et al.* [11] announced a simple cubic (sc) or body-centered-cubic (bcc) structure, while Wu *et al.* [12] find

*Author to whom correspondence should be addressed. Electronic address: jean.peyrelasse@univ-pau.fr

a face-centered-cubic (fcc) structure. On the other hand, Ivanova *et al.* [19] show the possibility of transitions from spherical micelles in bcc structure to hexagonally packed cylindrical micelles. The purpose of our work is to carry out a complete study of three PEO-PPO-PEO copolymers in aqueous solution. The first two, Tetronic T908 and T704, are four-branched star copolymers consisting of PEO and PPO blocks fixed on an ethylene diamine; the last is the Pluronic P105 $(EO)_{37}(PO)_{56}(EO)_{37}$, which is a linear copolymer. We carried out rheological and small-angle neutron scattering studies on these copolymer solutions.

Rheological measurements can be used to determine the complex modulus of elasticity $G^*=G'+jG''$ as a function of angular frequency ω, strain γ, stress σ, and temperature T. By thermomechanical analysis (measurement of G^* according to temperature) we determined the various temperatures of transition. Then, small-angle neutron scattering performed on samples under flow and true crystallographic arguments make it possible to determine in a rigorous way the nature of the condensed phases. For the T908 solutions there is only one transition between the micellar solution and the crystalline phase which is bcc. T704 presents a transition between a micellar solution and a lamellar phase, then at higher temperatures a symmetrical transition, from lamellar phase to micellar solution. P105 has a more complex behavior since it presents several transitions: micellar solution to hexagonal phase, hexagonal phase to bcc crystals, bcc crystals to lamellar phase. In this latter case, the transitions from one phase to another appear in a narrow interval of temperature.

II. EXPERIMENT

A. Samples

Tetronics are four branched copolymers, in which each branch has the structure $(EO)_x$- $(PO)_y$ where EO and PO are, respectively, ethylene oxide and propylene oxide. A PO unit links the four branches to an ethylene diamine. For this study we used two Tetronic: T908 for which the numbers of EO and PO units per branch are, respectively, $x=114$ and $y=21$ and T704 for which $x=16$ and $y=18$. We also studied solutions of Pluronic P105 $(EO)_{37}(PO)_{56}(EO)_{37}$. The polymers were obtained from BASF and were used as received without further purification. The polymer concentration is expressed in weight percentage. Aqueous solutions were prepared by stirring at low temperature ($T=5\,^\circ$C) where water is a good solvent for both the PEO and PPO blocks. We used bidistilled water for all rheological experiments and deuterated water for the small-angle neutron scattering studies.

B. Techniques

We used a strain-imposed rheometer (ARES from Rheometric Scientific) equipped with a Couette geometry (cup diameter 34 mm, gap width 1 mm, inner height 33.4 mm). For all the thermomechanical analysis, the oscillatory angular frequency was kept constant at 10 rad s^{-1} and the strain was fixed at 1%. The sample was heated at a constant rate of $2\,^\circ$C min^{-1}. In order to avoid any preshear of the sample, the following procedure was adopted. The solution was inserted in the precooled cup ($5\,^\circ$C), so that the sample was liquid, and after introduction of the rotor it was covered by a thin layer of low viscosity silicon oil to minimize evaporation of water.

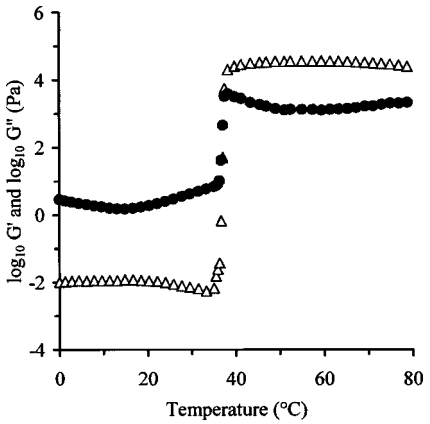

FIG. 1. Variations of G'' (•) and G' (△) with temperature for a 30% Tetronic T908 solution.

SANS experiments were performed at the Léon Brillouin Laboratory, CEA de Saclay (France) on the PAXY spectrometer. A wavelength of 6 Å was selected. The distance between the sample and detector was 3.2 m; this allowed a q range of 0.1–1.2 nm^{-1}. For the measurements on samples at rest, we used quartz cells with 2 mm path length. For the measurements under shear, we used a thermostatted Couette cell. The walls of the cell were made of quartz, and the external cylinder was mobile ($\Phi=47.24$ mm), while the internal cylinder ($\Phi=43.43$ mm) was fixed. The height of the inner cylinder was 55 mm. With respect to the cell, the shear rate $\dot{\gamma}$ could vary from 0 to 955 s^{-1}. In a neutron scattering experiment, the scattered intensity I is measured according to the scattering angle θ that is related to the scattering wave vector:

$$q=(4\pi/\lambda)\sin(\theta/2), \tag{1}$$

where λ is the wavelength of the neutron beam. Data collection is done in a two-dimensional (2D) detector that counts the number of scattered neutrons during a given time. A 2D scattering pattern is obtained and the one-dimensional $I(q)$ data set is generated by circular integration of the corresponding two-dimensional patterns.

III. RESULTS

A. Rheological measurements

Figures 1–3 show examples of the variations, according to the temperature, of the elastic modulus G' and of the loss modulus G'' of the three copolymer solutions studied. For the 30% solution of T908 only one transition is observed. It begins at $36\,^\circ$C and resembles a sol-gel transition. It corresponds to the transformation of the micellar solution into a crystalline phase. In the case of the 50% solution of T704 two transitions are observed: the first, which is sol-gel-like, at $26\,^\circ$C and the second, at $53\,^\circ$C, which corresponds to the melting of the "gel." In this case the gel zone is a peninsula

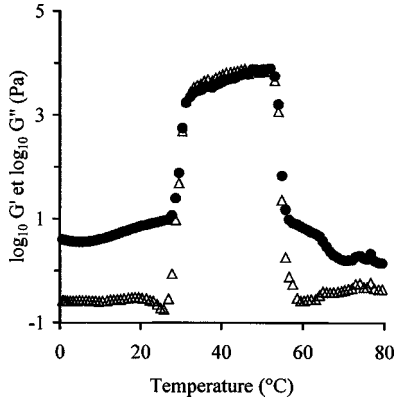

FIG. 2. Variations of G'' (•) and G' (△) with temperature for a 50% Tetronic T704 solution.

in the temperature-concentration phase diagram. For the 30% solution of P105, very clear transitions are detected at four temperatures: 20, 47, 54, and 72°C (the beginning of phase separation with clouding appears at 81°C). The first transition, as in the two preceding cases, resembles a sol-gel transition. It should be noted in Figs. 1–3 that in all cases the transitions appear in a narrow interval of temperature of about 3–4°C. By changing the concentration, we determined in the phase diagram the limits of the gel phases which are represented in Figs. 4–6. In the case of the solutions of P105, we added in Fig. 6 the temperatures at which the various transitions were observed. It should be noted that rheology cannot provide any information on the nature of the observed transitions. SANS experiments performed at carefully selected temperatures in the various temperature ranges can determine the exact nature of these transitions.

B. SANS measurements

1. SANS measurements on samples at rest

For the three systems studied, we carried out SANS measurements according to the temperature at different concentration. In all cases, at low temperature the scattered intensity remains weak but, above all, was independent of q. When the

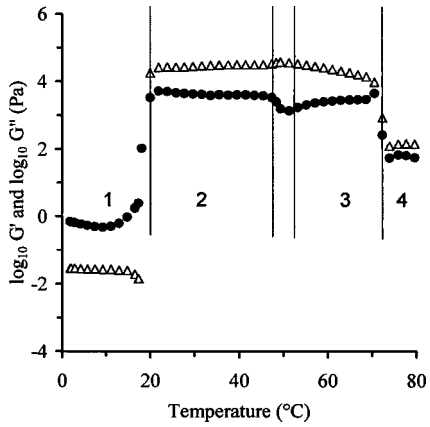

FIG. 3. Variations of G'' (•) and G' (△) with temperature for a 30% Pluronic P105 solution.

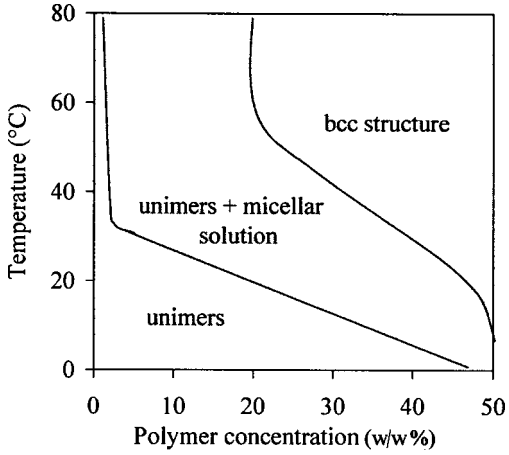

FIG. 4. Phase diagram of T908 solutions.

polymer is not micellized the solutions behave as a homogenous mixture. For higher temperature, a peak appears on the $I(q)$ spectra at the critical micellization temperature (TMC). This peak is due to significant intermicellar correlations, and its intensity increases with the volume fraction of micelles. The TMC lines are shown in Figs. 4–6. The goal of this article is not the study of the liquid micellar solutions. We proposed in a previous paper [28] for solutions of T908 a model which makes it possible to determine the radius of the micelles, their volume fraction, and their aggregation number as well as the fraction of unimers in equilibrium with the micelles. In the gel-like zones, the 2D pattern remains isotropic, but the $I(q)$ curve shows that the principal peak becomes thinner. We also note in some cases the existence of secondary Bragg peaks showing a transition to a liquid crystal structure. Figures 7 and 8 give two examples. Figure 7 represents the result obtained with a 30% solution of T908 at 45°C. If q_1, q_2, and q_3 are the q values of the successive peaks, the ratios q_3/q_1 and q_2/q_1 are roughly equal to $\sqrt{3}$ and $\sqrt{2}$. This shows that the structure is sc or bcc. It cannot be a fcc structure since in this case one would have $q_3/q_1=\sqrt{\frac{8}{3}}$ and $q_2/q_1=\sqrt{\frac{4}{3}}$.

For the 30% solution of P105 in zone 2 of Fig. 3, we note the existence of a small secondary Bragg peak at q_2, but the exact position of this peak is difficult to determine accurately (Fig. 8). In zone 3, only the main peak is highlighted. In zone

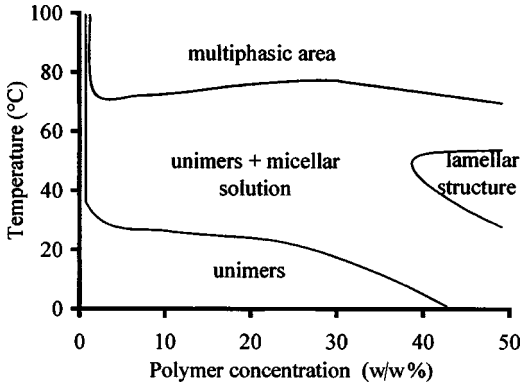

FIG. 5. Phase diagram of T704 solutions.

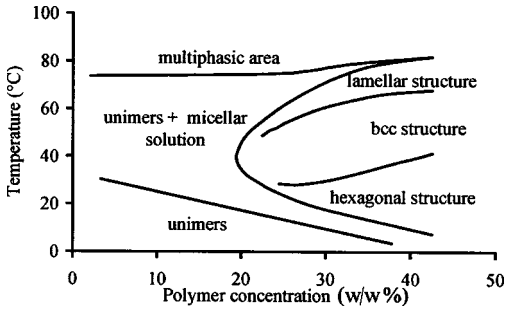

FIG. 6. Phase diagram of P105 solutions.

4 the small peak at $q_2=2q_1$ shows that the structure is probably lamellar. These results are equivalent to those obtained in a classical x-ray crystal powder experiment and clearly indicate, since the 2D pattern is isotropic, that the crystals exhibit all possible orientations in space. As a conclusion, it is obvious that SANS measurements conducted on samples at rest cannot provide sufficient information about the structure of these condensed phases.

2. SANS measurements on samples under flow

As SANS measurements conducted on samples at rest cannot characterize the structure of the condensed phases, we used SANS measurements on samples under flow as in a previous paper [29]. It is now well established that PEO-PPO-PEO crystalline structures can orient themselves when they are subjected to a shear [7,9–11]. Analogous behaviors have been reported for other ordered block polymer solutions [31,32,35,36]. When they are correctly analyzed, the diffraction patterns make it possible to determine the structure of the ordered phase and also the type of orientation.

When a solution in the gel-like state is subjected to a shear, spots are observed to appear on the 2D pattern. These spots become increasingly intense when the shear rate $\dot{\gamma}$ is increased. This result is general and was observed with all the samples studied in this work. At a low shear rate, the ring pattern of the unsheared sample coexists with broad peaks having a banana shape. When increasing the shear rate, the peaks become sharper, and the isotropic part of the scattered intensity disappears (see Figs. 9–13). We observed that there is a limit value of $\dot{\gamma}$ above which no further significant modification of the diffraction pattern is noted. It is important to note that there is no change in the position of the rings in the

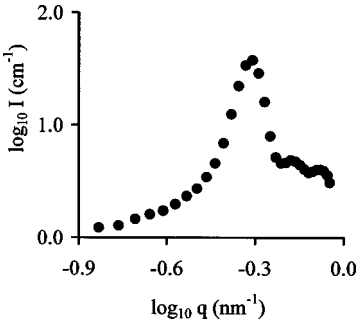

FIG. 7. Scattered intensity I according to the modulus q of the wave vector. 30% solution of Tetronic T908 at $T=45°C$.

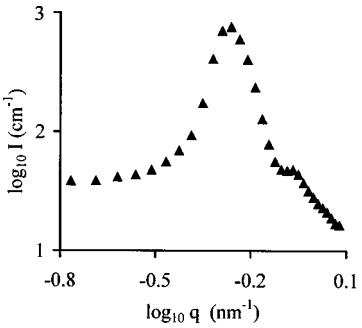

FIG. 8. Scattered intensity I according to the modulus q of the wave vector. 30% solution of Pluronic P105 at $T=30°C$ (zone 2 of Fig. 3).

case of T908 solutions—for instance, the ratios q_3/q_1 and q_2/q_1 of the peaks observed at rest are roughly equal to $\sqrt{3}$ and $\sqrt{2}$ (cubic lattice), and it is the same for the oriented samples. So the transition was gradually from a powder-like sample to a sample with complete alignment, but the crystalline structure is the same one. Moreover, no distortion of the crystalline structure is observed. When the sample is completely aligned one does not observe any further modification of the diffraction pattern up to the maximum shear rates accessible with our experimental setup (955 s^{-1}). In all cases, it was also noted that, when at rest, a preoriented sample does not present any disorientation process even after a long period of time ($t>10$ hs). Figures 11–13, show the different diffraction patterns obtained under flow with the 30% solution of P105 for temperatures chosen in zones 2, 3, and 4 of Fig. 3.

The case of the solutions of T704 between 29°C and 53°C (Fig. 10) and P105 in zone 4 (Fig. 13) is easy to interpret. The patterns are characteristic of lamellar structures. Figure 13 shows that a secondary peak appears clearly for a value of q which is equal to twice that of the main peak. For the solution of T704 the secondary peak is not highlighted, but only because of the experimental limits at high values of q.

For the other cases, Figs. 9, 11, and 12 show that the diffraction spots are distributed in vertical and equidistant layers, as well as in concentric circles: they resemble an

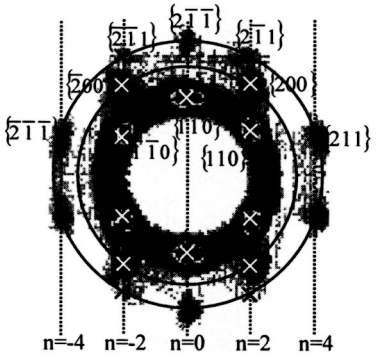

FIG. 9. 2D experimental pattern of a 30% solution of Tetronic T908 under flow at 45°C with $\dot{\gamma}=500$ s^{-1}. The crosses show the theoretical spots of a bcc lattice oriented with the row [1,1,1] in the flow direction, but random position about this direction.

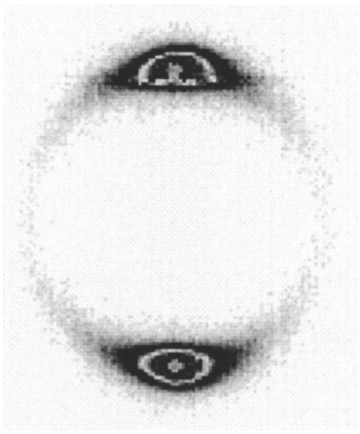

FIG. 10. 2D experimental pattern of a 50% solution of Tetronic T704 under flow at 45°C and with $\dot{\gamma}=30\ s^{-1}$.

x-ray diffraction diagram obtained by the crystal rotation method. We will review the known results of this classic method.

IV. DISCUSSION

A. Crystal rotation method

A monocrystal with an unspecified position related to an incidental beam does not emit any diffracted rays, since the Bragg relation is not necessarily satisfied. It will be recalled that if θ is the scattering angle, a reticular plane of Miller indices $\{h,k,l\}$ emit a diffraction ray if the reticular distance d_{hkl} satisfies the well-known Bragg relation

$$2d_{hkl}\sin(\theta/2)=\lambda. \tag{2}$$

In order to obtain a complete pattern of diffraction, it is necessary to rotate the sample around the direction $[u,v,w]$ of the crystal. During the rotation, each reticular plane having an angle to the incident beam that satisfies the Bragg relation makes possible a reflection. The result is a spot diagram. The diffraction spots are distributed on parallel layers and on concentric circles. If the $[u,v,w]$ axis of rotation is

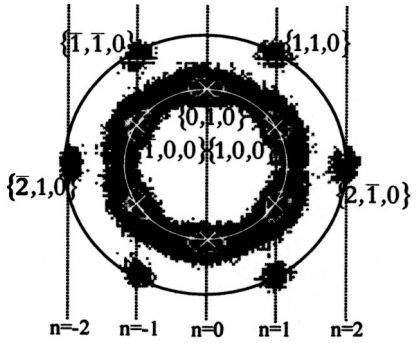

FIG. 11. 2D experimental pattern of a 30% solution of Pluronic P105 under flow at 40°C and with $\dot{\gamma}=60\ s^{-1}$ (zone 2 of Fig. 3). The crosses show the theoretical spots of a hexagonal lattice oriented with the row $[1,0,0]$ in the flow direction, but random position about this direction.

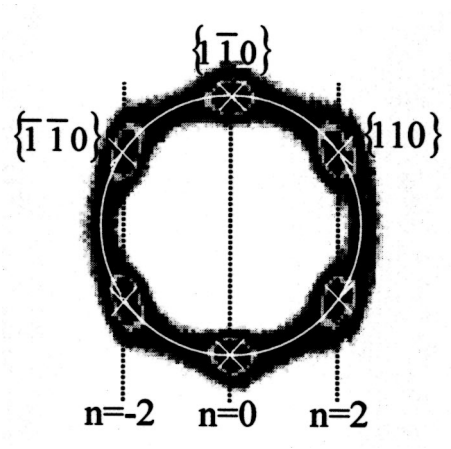

FIG. 12. 2D experimental pattern of a 30% solution of Pluronic P105 under flow at 60°C and with $\dot{\gamma}=450\ s^{-1}$ (zone 3 of Fig. 3). The crosses show the theoretical spots of a bcc lattice oriented with the row $[1,1,1]$ in the flow direction, but random position about this direction.

perpendicular to the incidental beam, the spots from the layer of order n satisfy the following equation:

$$uh+vk+wl=n. \tag{3}$$

The first layers are equidistant and have a gap Δ given by

$$\Delta=\frac{D\lambda}{L}, \tag{4}$$

where D is the distance between the sample and the detector and L the distance between two consecutive nodes on the $[u,v,w]$ row. If the rotation row is horizontal, the layers will be vertical and on the same circle of radius r one will find the diffraction spots due to reticular planes having the same d_{hkl} since they will have the same diffraction angle [Eq. (2)]. It is easy to check that when the diffraction

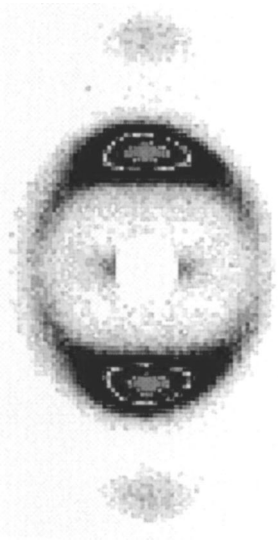

FIG. 13. 2D experimental pattern of a 30% solution of Pluronic P105 under flow at 75°C and with $\dot{\gamma}=10\ s^{-1}$ (zone 4 of Fig. 3).

angles are small, r is proportional to q and inversely proportional to d_{hkl} (tan $\theta = r/D$). It is also possible to calculate the angular positions of the spots on the 2D diffraction pattern. Let us consider the spot of the reticular plane $\{h,k,l\}$ on the xth layer and on the circle of radius r. The angle α between the direction passing by this spot and the center of the diagram and the vertical direction is given by $\sin \alpha = x\Delta/r$. As $\tan \theta = r/D$, with the Bragg relation and the expression of Δ given by Eq. (4), since the angles are small, we obtain

$$\sin \alpha = x\frac{d_{hkl}}{L}. \tag{5}$$

Knowing the row around which rotation is carried out, it is possible theoretically to build the diffraction pattern of various crystalline structures. We will limit our comments to some particular cases that will be useful for the continuation of the discussion.

1. bcc lattice

Let us first consider a bcc monocrystal whose rotation is carried out around the $[1,1,1]$ row. For the cubic lattices of cell parameter a, $d_{hkl} = a/(\sqrt{h^2+k^2+l^2})$, and for the bcc lattice, the sum $h+k+l$ must be even. The first circle of radius r_1 will present the spots due to the reflections by reticular planes of $\{1,1,0\}$ type and the following concentric circles (radius $r_2, r_3, \ldots$) will show reflections by the planes $\{2,0,0\}, \{2,1,1\}, \ldots$. The ratios of the radius $r_3/r_1 = d_{110}/d_{211}$ and $r_2/r_1 = d_{110}/d_{200}$ are, respectively, equal to $\sqrt{3}$ and $\sqrt{2}$.

The layer $n=0$ $(h+k+l=0)$ will contain the spot $(1,\bar{1},0\}$ on the circle of radius r_1 and the spot $\{1,1,\bar{2}\}$ on the circle r_3. The layer $n=2$ $(h+k+l=2)$ will contain successively the spots $\{1,1,0\}$, $\{2,0,0\}$, and $\{2,\bar{1},1\}$ on the three circles. On the layer $n=4$ $(h+k+l=4)$, the spot $\{2,1,1\}$ will be found on the circle of radius r_3. It is possible to continue the reasoning for higher values of n, but this is not useful for the continuation of our discussion.

It is then possible to predict the angular positions of the different spots with Eq. (5). For the spot $\{1,1,0\}$, $x=1$, $d_{hkl} = a/\sqrt{2}$. The periodicity L along the row $[1,1,1]$, which is the diagonal of the cube, is equal to $a\sqrt{3}/2$, which leads to $\sin \alpha = 2/\sqrt{6}$—that is to say, $\alpha = 54.7°$. The six spots of the first circle are thus separated by four angles of 54.7° and two angles of 70.5°. In the same way it is possible to calculate the angular positions of the spots of the second and third circles.

2. Hexagonal lattice

The hexagonal lattice is built on two equal vectors ***a*** and ***b*** forming an angle of 120° and on a vector ***c*** perpendicular to the plane of ***a*** and ***b***. This network has a symmetry axis of order 6. The reticular distances are given by

$$d_{hkl} = \frac{a}{\sqrt{\frac{4}{3}(h^2+k^2+hk)+\frac{l^2a^2}{c^2}}}. \tag{6}$$

Indeed, d_{hkl} depends on the a/c ratio; it is not possible for this network to give a list of the reticular planes by order of decreasing spacing as in the case of the cubic lattices. However, the reticular distances for the smallest Miller indices are given by $d_{100} = a\sqrt{3}/2$, $d_{110} = a/2$, $d_{200} = a\sqrt{3}/4$, $d_{001} = c$, and $d_{002} = c/2$. If the spots of d_{100} type are on a circle of radius r_1, the spots d_{110} will be on a circle of radius $r_2 = r_1\sqrt{3}$, the spots d_{200} on the circle of radius $r_3 = 2r_1$. The spots d_{001} and d_{002} will be, respectively, on the circles of radii $(\sqrt{3}/2)(a/c)r_1$ and $\sqrt{3}(a/c)r_1$. It will be observed that when $c \gg a$, these reticular planes do not give any visible diffraction spots.

We assume that rotation of the monocrystal is carried out around the row $[1,0,0]$ and that $c \gg a$. On the equatorial layer $(n=0)$, the spot $\{0,1,0\}$ will be located on the circle of radius r_1. On the second layer $(n=1)$, the spot $\{1,0,0\}$ will be located on the circle of radius r_1 and the spot $\{1,\bar{1},0\}$ on the circle of radius r_2. On the layer $n=2$, the spot $\{2,\bar{1},0\}$ will be on the circle of radius r_2 since $d_{2\bar{1}0} = d_{110}$. The spot $\{2,0,0\}$ will be on the same layer but on the circle of radius r_3.

One can define the angular positions of the spots on the diffraction diagram using Eq. (5). For the hexagonal network, the periodicity along the row $[1,0,0]$ is equal to a. For the spot $\{1,0,0\}$, $x=1$, $d_{100} = a\sqrt{3}/2$, one obtains $\alpha = 60°$. For the spot $\{1,1,0\}$, $x=1$, $d_{110} = a/2$—that is to say, $\alpha = 30°$. For the spot $\{2,\bar{1},0\}$, $x=2$, $d_{2\bar{1}0} = a/2$, which leads to $\alpha = 90°$.

B. Interpretation of the results

We have constructed in Fig. 9 the theoretical diffraction pattern for a rotating crystal experiment when the crystal is bcc and when the axis of rotation is a horizontal $[1,1,1]$ row. The radius of the circle, r_1, was simply adjusted in order to obtain the same scale as the experimental one. It is easy to check that for the solutions of T908, the theoretical diffraction pattern for the bcc network is exactly superposable with the experimental one. All theoretically predicted spots are highlighted up to diffraction $\{2,1,1\}$. The experimental result obtained without any rotation of the sample is identical to that using a monocrystal rotated around the $[1,1,1]$ direction. This is the proof that the bcc polycrystals, which exhibited all possible orientations in space in an experiment at rest (the diffraction patterns are powder-like), now orient with shearing, with the $[1,1,1]$ direction along the flow direction but with random orientation about this direction.

Knowing now that the network is bcc, it is possible to calculate the cell parameter a. With the Bragg relation and the definition of q, if one designates by q_1 the value of q corresponding to the spots $\{1,1,0\}$, one obtains $a = 2\pi\sqrt{2}/q_1 = 180$ Å. If it is assumed that the spherical micelles are in compact packing along the diagonal of the cube, one obtains a radius of 78 Å at a temperature of 38 °C. For the same solutions in the liquid zone at 30 °C, we calculated [28] a micelle radius of 66 Å. This shows that the micelles are not in compact packing along the dense direction of the network.

With regard to the P105, in zone 3 of Fig. 3, the diffraction pattern revealed only one series of spots distributed on

the same circle. Figure 12 shows that the micelles are ordered in a bcc lattice. However, contrary to the case of T908 solutions, the diffractions $\{2,0,0\}$ and $\{2,1,1\}$ are not highlighted. It does not seem that it is because of a poor orientation of the crystals, since the peaks are as intense and well defined as in the case of T908. A possible explanation could be that the size of the crystals is smaller.

For the solution of P105, in zone 2, the theoretical diffraction pattern obtained for a hexagonal network is exactly superposable with the experimental one (Fig. 11). This makes it possible to conclude that the system is composed of cylindrical micelles of length $c \gg a$. The crystals are oriented with the row $[1,0,0]$ in the flow direction. However, crystals having all the orientations around $[1,0,0]$ are present in the sample. The cell parameter is given by $a=4\pi/q_1\sqrt{3}$ where q_1 is the q position of the $\{1,0,0\}$ spots. This leads to $a=140$ Å, and its variation with the temperature is low. If we assume that the cylinders are in compact packing in the $\{0,0,1\}$ plane, we can estimate their radius at 70 Å.

Eiser *et al.* [7] obtained with Pluronic F108 solutions, at rest and for small shear rates, a small-angle x-ray scattering (SAXS) pattern that is powder-like, with three rings of radius r_1, r_2, and r_3. The r_3/r_1 and r_2/r_1 ratios are very close to 1.7 and 2 as predicted for the hexagonal structure. Moreover, for high shear rates, they obtained a diffraction pattern that is very close to the one represented in Fig. 11. All these results seem to suggest a hexagonal structure instead of fcc as announced by the authors. In the same way, the diffraction pattern of solutions under flow of F127 allotted by Mortensen [10] to a body-centered network is probably that of a hexagonal structure, since the spots of the first two rings are separated by angles of 60° as in Fig. 11.

The 50% solution of T704 between 29°C and 53°C and that of P105 in zone 3 form lamellar structures. The periodicity is given by $e=2\pi/q_1$. For the T704 solutions, a small linear increase of e is observed with increasing temperature since $e=73$ Å at 29°C and 82 Å at 53°C. The periodicity for the lamellas formed by the P105 is much larger: $e=145$ Å.

Our study shows that the copolymer solutions studied form polycrystals which exhibited, at rest, all possible orientations in space since the 2D pattern is isotropic. The polycrystals orient with shearing, with a particular direction along the flow direction but with random orientation about this direction. Our results are not in contradiction with those of other groups, but show that the type of alignment under shear depends on the system studied. The work of Hamley *et al.* [32] for $E_{86}B_{10}$ is characteristic. After orientation of the sample by large-amplitude shearing at high frequency, these authors determine the diffraction pattern for different angles of rotation around the $[1,1,1]$ direction. For some angles of rotation, the figure obtained is poor, but by superposition of the different patterns, it is easy to verify that an exact match with Fig. 9 is obtained. Unlike our system for which the crystals can present all orientations around the principal direction $[1,1,1]$, Hamley *et al.* obtained a near perfect single-crystal alignment. The rotation around $[1,1,1]$ brings the observed $\{1,1,0\}$, $\{2,0,0\}$, $\{2,1,1\}$, and $\{2,2,0\}$ reflections into the Bragg diffracting conditions. Many authors have explained their diffraction figures by considering the existence of twinned structures. In the case of the diblock polymer solutions of polystyrene/polyisoprene in decane, McConnell *et al.* [35] show that the bcc crystal is twinned with the twinning plane perpendicular to the $\{1\,1\,0\}$ planes and the twins are oriented at 35.3° with respect to the shear direction. Similar explanations have been suggested by Hamley *et al.* [36] for aqueous solutions of poly(oxyethylene)-poly(oxybutylene), $E_{210}B_{16}$. In the case of the solutions that we studied, true crystallographic arguments allow an interpretation of the diffraction pattern without any allusion to twinned structures. It is also possible to find examples in which the hypothesis of a more favorable direction allows an interpretation of all the observed spots. However, some spots predicted by the laws of crystallography remain absent. This indicates that all crystals have a common direction but some orientations around this common direction are not present in the sample. This is probably the case of the F68 solutions studied by Eiser *et al.* for which the spots $\{1,\bar{1},0\}$ and $\{2,\bar{1},1\}$ of the bcc lattice are not detected [9]. It can be noted that this phenomenon is often observed for laminated metals.

V. CONCLUSIONS

Block copolymers in aqueous solutions are likely to present condensed phases which are liquid crystals. In this article we showed that transitions between various nanostructures can occur at fixed concentration, during a temperature sweep. This explains the apparent contradiction that one can find in the literature if the studies are carried out at different temperatures and concentrations. It is possible to determine these transition temperatures by rheological analysis. SANS performed on samples under flow provide characteristic diffraction patterns and true crystallographic analysis makes it possible to identify the various nanostructures. We show that the polycrystals, which exhibited all possible orientations in space in an experiment at rest, orient with shearing, with a particular direction along the flow direction but with random orientation about this direction.

[1] L. Yang, P. Alexandridis, D. C. Steytler, M. J. Kositza, and J. F. Holzwarth, Langmuir **16**, 8555 (2000).
[2] K. Mortensen, J. Phys.: Condens. Matter **8**, A103 (1996).
[3] I. Goldmints, G. Y. Yu, C. Booth, K. A. Smith, and T. A. Hatton, Langmuir **15**, 1651 (1999).
[4] I. Goldmints, F. K. von Gottberg, K. A. Smith, and T. A. Hatton, Langmuir **13**, 3659 (1999).
[5] Y. C. Liu, S. H. Chen, and J. S. Huang, Phys. Rev. E **54**, 1698 (1996).
[6] K. Mortensen, Colloids Surf., A **183**, 277 (2001).

[7] E. Eiser, F. Molino, and G. Porte, Eur. Phys. J. E **2**, 39 (2000).
[8] E. Eiser, F. Molino, G. Porte, and O. Diat, Phys. Rev. E **61**, 6759 (2000).
[9] E. Eiser, F. Molino, G. Porte, and X. Pithon, Rheol. Acta **39**, 201 (2000).
[10] K. Mortensen, Polym. Adv. Technol. **12**, 2 (2001).
[11] R. K. Prud'homme, G. Wu, and D. K. Schneider, Langmuir **12**, 4651 (1996).
[12] C. Wu, T. Liu, B. Chu, D. K. Schneider, and V. Graziano, Macromolecules **30**, 4574 (1997).
[13] G. Schmidt, W. Richtering, P. Lindner, and P. Alexandridis, Macromolecules **21**, 2293 (1998).
[14] P. Alexandridis and L. Yang, Macromolecules **33**, 3382 (2000).
[15] C. Guo, H. Z. Liu, and J.-Y. Chen, Colloids Surf., A **175**, 193 (2000).
[16] B. Chu, G. Wu, and D. K. Schneider, J. Polym. Sci., Part B: Polym. Phys. **32**, 2605 (1994).
[17] R. Ivanova, B. Lindman, and P. Alexandridis, Adv. Colloid Interface Sci. **89-90**, 351 (2001).
[18] P. Alexandridis and L. Yang, Macromolecules **33**, 5574 (2000).
[19] R. Ivanova, B. Lindman, and P. Alexandridis, Langmuir **16**, 9058 (2000).
[20] G. Wu, L. Liu, V.-B. Buu, B. Chu, and D. K. Schneider, Physica A **231**, 73 (1996).
[21] L. Guo, R. H. Colby, M. Y. Lin, and G. P. Dado, J. Rheol. **45**, 1223 (2001).
[22] R. Ivanova, P. Alexandridis, and B. Lindman, Colloids Surf., A **183–185**, 41 (2001).
[23] P. R. Desai, N. J. Jain, R. K. Sharma, and P. Bahadur, Colloids Surf., A **178**, 57 (2001).
[24] N. J. Jain, V. K. Aswal, P. S. Goyal, and P. Bahadur, Colloids Surf., A **173**, 85 (2001).
[25] K. Mortensen, W. Brown, and E. Jorgensen, Macromolecules **27**, 5654 (1994).
[26] K. Mortensen, Macromolecules **30**, 503 (1997).
[27] Z. Zhou and B. Chu, Macromolecules **27**, 2025 (1994).
[28] C. Perreur, J. P. Habas, J. Peyrelasse, J. François, and A. Lapp, Phys. Rev. E **63**, 031505 (2001).
[29] C. Perreur, J. P. Habas, J. François, J. Peyrelasse, and A. Lapp, Phys. Rev. E **65**, 041802 (2002).
[30] E. Beaudoin, O. Borisov, L. Billon, R. Hiorns, and J. François, Macromolecules **35**, 7436 (2002).
[31] C. Daniel, I. W. Hamley, M. Wilhelm, and W. Mingvanish, Rheol. Acta **40**, 39 (2001).
[32] I. W. Hamley, J. A. Pople, J. P. A. Fairclough, A. J. Ryan, C. Booth, and Y.-W. Yang, Macromolecules **31**, 3906 (1998).
[33] M. E. Vigild, K. Almdal, K. Mortensen, I. W. Hamley, J. P. A. Fairclough, and A. J. Ryan, Macromolecules **31**, 5702 (1998).
[34] C.-Y. Wang and T. P. Lodge, Macromolecules **35**, 6997 (2002).
[35] G. A. McConnell, M. Y. Lin, and A. P. Gast, Macromolecules **28**, 6754 (1995).
[36] I. W. Hamley, K. Mortensen, G.-E. Yu, and C. Booth, Macromolecules **31**, 6958 (1998).